



# An air-stable, aluminium-based ionic liquid electrolyte for energy storage†

 Matthew Stalcup, Mia Blea, Elena Medina, Stephen J. Percival \* and Erik D. Spoecke \*

 Cite this: *Chem. Commun.*, 2025, 61, 5657

 Received 30th September 2024,  
 Accepted 19th February 2025

DOI: 10.1039/d4cc05163g

rsc.li/chemcomm

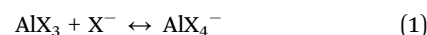
**High capacity, lightweight multivalent aluminum (Al) is attractive as an energy storage active material. Current Al containing electrolytes are prohibitively air/moisture sensitive and do not cycle under ambient conditions. Here, promising, reversible electrochemical behavior of Al-containing, air-stable ionic liquids is demonstrated through the addition of the Lewis-base complexing agent, NaI.**

The electrochemical reduction of aluminum chloride in room temperature ionic liquid-based electrolytes has been explored as a possible method for plating metallic aluminum,<sup>1,2</sup> a goal with implications for energy storage. These systems typically consist of a chloroaluminate salt and a chloride-containing ionic liquid (IL) that form reactive Lewis acid/base complexes.<sup>1</sup> Limiting the practical use of such electrolytes, though, is their sensitivity to air and water, necessitating the use of inert atmospheres.<sup>1,3</sup> Here, we aim to enable reversible electrochemical oxidation and reduction of an Al-based active species in an (IL) that is air-stable under ambient conditions.

Arguably the most studied Al-based IL electrolyte consists of aluminium chloride (AlCl<sub>3</sub>) and 1-ethyl-3-methylimidazolium chloride (EMIM[Cl]).<sup>4–6</sup> This system is highly unstable under an open atmosphere and requires that experiments be performed in a glovebox to maintain electrochemical stability.<sup>3,7,8</sup> Prior reports on these systems, however, reveal critical details about how the electrolyte speciation can dramatically affect the electrochemical behaviour of the system. Notably, the Lewis acid/base relationship in the electrolyte is critical in the formation of reducible aluminium halide (AlX<sub>3</sub>) species.<sup>3,9</sup>

In Lewis basic solutions the AlX<sub>3</sub> mole fraction is less than 0.5 with the majority species being AlX<sub>4</sub><sup>−</sup> (eqn (1)), which is not typically considered electrochemically active in Cl<sup>−</sup>-based electrolytes.<sup>2,7</sup> When more AlX<sub>3</sub> is added to achieve an overall Lewis acidic solution/melt, a chloroaluminate dimer (Al<sub>2</sub>X<sub>7</sub><sup>−</sup>) is

formed (eqn (2)). This dimer complex is central to the electrochemical reduction of aluminium from ILs (eqn (3)).<sup>3,5</sup>



To address the impractical air and moisture sensitivity of these active species, alternative anions (X) may be considered in place of Cl<sup>−</sup>. For example, bis[(trifluoromethyl)sulfonyl]imide (TFSI) is a large, hydrophobic anion that can undergo ligand exchange with the AlCl<sub>3</sub> species. Strong binding of the large, sterically-limiting TFSI<sup>−</sup> to the Al<sup>3+</sup> results in relatively more stable complexes, but these species are difficult to reduce electrochemically.<sup>10,11</sup>

To overcome this challenge, we introduced iodide (I<sup>−</sup>) (as sodium iodide (NaI)) into an AlCl<sub>3</sub>/EMIM[TFSI] system to modify the Al-dimer complexation and *promote the formation of electrochemically active Al species while remaining air stable*. We hypothesized that introducing a Lewis base (such as I<sup>−</sup>), to the AlCl<sub>3</sub>/EMIM[TFSI] melts would stabilize the electrochemically active Al complex and prevent the bulky TFSI from strongly coordinating the Al ions. Similar effects have been reported when adding Li<sup>+</sup> to stabilize Mg cycling electrochemistry.<sup>12</sup>

Raman spectroscopy was used to assess and compare speciation in the electrolyte for EMIM[TFSI], AlCl<sub>3</sub>/EMIM[TFSI], and AlCl<sub>3</sub>/EMIM[TFSI] with NaI (Fig. 1). Fig. 1A shows the baseline spectrum for EMIM[TFSI] and the impact of adding AlCl<sub>3</sub> to the system. The spectra show EMIM[TFSI]-related peaks between 200 and 650 cm<sup>−1</sup> in the blue curve.<sup>11,13</sup> Select TFSI-specific peaks drop dramatically with the addition of 2 M AlCl<sub>3</sub>, and they are nearly entirely eliminated with the 5 M AlCl<sub>3</sub>. These drops, combined with the emergence of a peak attributable to the extreme binding case of Al[TFSI]<sub>3</sub> near 760 cm<sup>−1</sup> indicate strong TFSI<sup>−</sup> anion complexation by Al-species as previously reported.<sup>11,14</sup> The 2 M AlCl<sub>3</sub> electrolyte also shows the emergence of a significant peak at 349 cm<sup>−1</sup>, corresponding to an AlCl<sub>4</sub><sup>−</sup> complex,<sup>15</sup> as predicted by eqn (1). (There are likely additional species where X may be a mix of Cl<sup>−</sup>

Sandia National Laboratories, Albuquerque, New Mexico 87185, USA.

 E-mail: [sperciv@sandia.gov](mailto:sperciv@sandia.gov), [edspoer@sandia.gov](mailto:edspoer@sandia.gov)

Tel: +1 (505) 845-0207, +1 (505) 284-1932

 † Electronic supplementary information (ESI) available: ESI contains experimental methods, SEM & EDX characterization of electrodeposited materials from electrolytes. See DOI: <https://doi.org/10.1039/d4cc05163g>




Fig. 1 (A) Raman spectra comparing the Aluminum halide complex speciation for the EMIM[TFSI] ionic liquid electrolyte and the impact of adding NaI (B).

and TFSI<sup>-</sup>, but these species are not clearly attributable in the Raman data.) With increased AlCl<sub>3</sub> in the 5 M electrolyte, the AlCl<sub>4</sub><sup>-</sup> complex is largely converted to Al<sub>2</sub>Cl<sub>7</sub><sup>-</sup> dimers (eqn (2)), indicated clearly by peaks at 259, and 305 cm<sup>-1</sup>. This observation is consistent with prior reports suggesting that electroactive dimer (Al<sub>2</sub>Cl<sub>7</sub><sup>-</sup>) formation is only present in at higher concentrations (*e.g.*, 5 M) in this ionic liquid.<sup>2,15</sup> (Much smaller dimer peaks appear to be present in the 2 M AlCl<sub>3</sub> electrolyte.)

Changes to the spectra in Fig. 1B, however, reveal different speciation when 1 M NaI is present in these AlCl<sub>3</sub>-based electrolytes. In the 2 M AlCl<sub>3</sub> sample, the TFSI peaks are much less diminished, suggesting more free, less complexed TFSI<sup>-</sup> anion than seen in Fig. 1A. There remains, however, a very strong AlCl<sub>4</sub><sup>-</sup> peak (348 cm<sup>-1</sup>) suggesting that significant chloride anions are being displaced, but not by TFSI anions. Rather, the softer iodide Lewis base is believed to preferentially coordinate with the Al-complex in place of the TFSI anions. Iodide-substituted AlCl<sub>4</sub><sup>-</sup> monomers, such as AlCl<sub>3</sub>I<sup>-</sup>, AlCl<sub>2</sub>I<sub>2</sub><sup>-</sup>, and AlClI<sub>3</sub><sup>-</sup> are known to form, though direct detection of identifying Raman peaks has only been reported at iodide mole fractions exceeding the solubility of NaI in this system.<sup>16</sup> In addition, previous reports have described dimeric species (*e.g.*, Al<sub>2</sub>Cl<sub>6</sub>I<sup>-</sup>), which are likely present here, as well.<sup>17</sup> Although these species (and possible mixed, TFSI-containing complexes) are not directly evident in Fig. 1, we can infer the coordination of the iodide from (1) the changes in AlCl<sub>4</sub><sup>-</sup> and TFSI<sup>-</sup> speciation with NaI addition, (2) the fact that the NaI is soluble in this electrolyte (at 1 M), but is *insoluble* in EMIM[TFSI] without AlCl<sub>3</sub> complexation, and (3) the iodide-specific impact on the electrochemical behavior of the Al-complexes shown below.

Notably, when the AlCl<sub>3</sub> concentration was increased to 5 M, the concentration of AlCl<sub>3</sub> overwhelmed the influence of the 1 M I<sup>-</sup> complexation, and the spectrum again shows loss of the TFSI<sup>-</sup> anion and growth of the Al<sub>2</sub>Cl<sub>7</sub><sup>-</sup> peaks as seen in Fig. 1A. In this 5 M concentration, coordinated anions in solution are expected to be a mix of Cl<sup>-</sup>, I<sup>-</sup>, and TFSI<sup>-</sup>, though not all species are visible in spectra of Fig. 1.

To assess the impact of this varied speciation on the system electrochemistry, we explored the electrochemical behaviour of the AlCl<sub>3</sub>/EMIM[TFSI] system at 2 different concentrations of

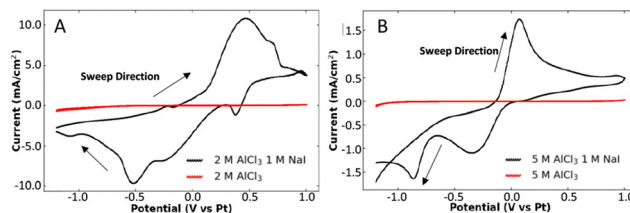


Fig. 2 Cyclic voltammograms (CVs) for EMIM[TFSI] electrolyte as affected by AlCl<sub>3</sub> and NaI. CVs shown for (A) 2 M AlCl<sub>3</sub> with and without 1 M NaI and (B) 5 M AlCl<sub>3</sub> with and without 1 M NaI. CVs were collected using a 3 mm Ni disk at 100 mV s<sup>-1</sup> with a platinum (Pt) wire quasi-reference electrode and a Pt wire counter electrode.

AlCl<sub>3</sub> (2 M and 5 M), with and without 1 M NaI addition. These tests were conducted *in open air under ambient conditions with approximately 50% atmospheric humidity*. Fig. 2A and B show representative cyclic voltammograms (CVs) (starting at a reducing potential) for these 4 test configurations and reveal the clear impact of NaI addition to the electrolyte.

In Fig. 2A, the 2 M AlCl<sub>3</sub> mixture shows no substantial reduction or oxidation peaks until the potential is swept to near the CV potential window limits. This result agrees with the Raman data indicating little of the electroactive dimer (Al<sub>2</sub>Cl<sub>7</sub><sup>-</sup>). It also confirms the relative electrochemical inactivity of the AlCl<sub>4</sub><sup>-</sup> and TFSI-coordinated complexes believed to be present.

In contrast, when NaI is added into the 2 M AlCl<sub>3</sub> system there is a substantial increase in the measurable electrochemical behaviour, and both reduction and oxidation peaks are present, indicating more active, reversible electrochemical species in the melt. Because NaI is insoluble in EMIM[TFSI] without the AlCl<sub>3</sub> present, the electrochemistry of NaI alone in the system could not be studied. Still, the increased electrochemical activity is clearly due to the collaborative influences of NaI and AlCl<sub>3</sub> in the hydrophobic EMIM[TFSI] system and allows for air and humidity-stable, reversible electrochemistry.

When the concentration of AlCl<sub>3</sub> is increased to 5 M (Fig. 1B), without the NaI additive, appreciable current is seen for the single reduction feature near -0.8 V, attributable to the more abundant dimer at this higher concentration. Lack of an oxidation peak, however, reveals that this reaction is not reversible. When NaI was present in the 5 M AlCl<sub>3</sub> electrolyte, the electrochemistry changed further, reminiscent of the 2 M AlCl<sub>3</sub> condition with NaI, complete with multiple reduction peaks as well as oxidation features.

Comparing the CV data to the Raman speciation results, we note first that the least electrochemically responsive EMIM[TFSI] electrolyte is that containing 2 M AlCl<sub>3</sub>, where minimal current is likely attributable to the limited Al<sub>2</sub>Cl<sub>7</sub><sup>-</sup> dimer formation and the likely complexing of the inactivating TFSI<sup>-</sup> anion to both the monomers and dimers. In contrast, the most electrochemically responsive, reversible EMIM[TFSI] electrolyte is the same 2 M AlCl<sub>3</sub> but with 1 M NaI present. This dramatic difference may be attributed to reduced TFSI<sup>-</sup> anion complexing of the limited dimer formation at this concentration of AlCl<sub>3</sub>, but it is more likely that the increased current and presence of multiple reversible oxidation and reduction peaks is attributable to iodide-coordinated (*e.g.*, AlCl<sub>3</sub>I<sup>-</sup>) species as well as Al<sub>2</sub>Cl<sub>6</sub>I<sup>-</sup> and possibly



$\text{Al}_2\text{Cl}_7^-$  dimers. These iodide-based species, particularly  $\text{AlCl}_3\text{I}^-$ , are known to be electrochemically active in other systems,<sup>17,18</sup> and could represent a new set of electroactive complexes for the EMIM[TFSI] system.

Considering the 5 M  $\text{AlCl}_3$  electrolytes, the system with no NaI shows limited electrochemical reduction, likely due to increased concentration of  $\text{Al}_2\text{Cl}_7^-$  dimers, but the evident binding of TFSI<sup>-</sup> to the aluminium chloride complexes still limited the current significantly. With the addition of 1 M NaI, reduction peaks emerge and grow (as do oxidation peaks) indicating that the iodide-substituted ligands do influence the electrochemistry, but the current of even these active species is much lower than in the 2 M  $\text{AlCl}_3$ , 1 M NaI case. Again, the relatively high concentration of electrochemically inactive (or minimally active)<sup>11</sup> TFSI-substituted complexes are believed to have diminished the electrochemical behaviour.

Additional details about the electrochemical processes in play are revealed by examining material deposited on the Ni foil electrodes when each system was “charged” by holding the electrolyte at a constant  $-1.2$  V vs. Pt (Pt counter and reference electrodes). Scanning electron micrographs (SEM) and energy dispersive X-ray analyses (EDX) (See Fig. S2–S6, ESI<sup>†</sup>) show that all samples that contained significant TFSI-substituted aluminium chloride complexes (2 M  $\text{AlCl}_3$ , 5 M  $\text{AlCl}_3$ , and 5 M  $\text{AlCl}_3$  with 1 M NaI), material deposits were found on the Ni foil. As highlighted in Fig. 3, the EDX spectra show that these deposits are rich in Al, Cl, C, and S.

We deduce from these data that the deposits are partially reduced aluminium chloride complexes, including TFSI-exchanged complexes. The 3-electron reduction of  $\text{Al}^{3+}$  to form Al does not appear to be a dominant process in this air-exposed system, however; rather, possibly because of electron delocalization in the complexes, the electrochemistry appears to favor partial Al reduction to uncommon oxidation states, such as those reported in the literature.<sup>19–23</sup> While this process yielded irreversible degradation products in most cases, for the highly electrochemically active 2 M  $\text{AlCl}_3$ , 1 M NaI system, no deposits were seen on the Ni foil indicating that the iodide-mediated electrochemically active species remain *soluble*. The addition of the iodide Lewis base, produces a new complex that appears to undergo a reversible, partial faradaic reduction of the  $\text{Al}^{3+}$  complex. The iodide-containing complex may serve to stabilize the complexed Al ion in the 2+ or 1+ oxidation state and remains soluble in the electrolyte. While these species

clearly do not favor efficient 3-electron Al metal deposition, the data show that *efficient, reversible charge storage is possible in the soluble, Al-based complexes of this air-stable electrolyte*. In particular, the likely activity of  $\text{AlCl}_3\text{I}^-$  and  $\text{Al}_2\text{Cl}_6\text{I}^-$  species shows these complexes to be new candidates for electroactivity in this EMIM[TFSI] IL electrolyte system.

Further electrochemical experiments were conducted to determine how the electrolyte performs under different current density requirements and select constant-current, potentiometric traces can be seen in Fig. 4A and B. As seen in Fig. 4A and B, without NaI, electrolytes yielded undesirable, high potentials, reflective of a highly resistive system, even at modest current densities of  $0.2$  mA  $\text{cm}^{-2}$ . (Higher current densities are possible with NaI – see Fig. 2 and Fig. S1, ESI<sup>†</sup>). In these 2 M  $\text{AlCl}_3$  tests, the total voltage difference between charge and discharge (reductive and oxidative currents) is high at  $\sim 1.8$  V. In the 5 M concentrations, the tests quickly reached the compliance voltage limit of  $\pm 1.5$  V.

When NaI was added to the  $\text{AlCl}_3$ /EMIM[TFSI] system, though, both reductive (0–15 min) and oxidative (15–30 min) currents were not only achievable (see CVs in Fig. 2), but the electrolytes exhibited much smaller voltage differences, as low as 0.2 V for a half cell with 2 M  $\text{AlCl}_3$ . The 2 M  $\text{AlCl}_3$  system with 1 M NaI shows stable electrochemistry over all the time scales and current densities up to  $0.5$  mA  $\text{cm}^{-2}$  (Fig. S1, ESI<sup>†</sup>). In 5 M  $\text{AlCl}_3$  with 1 M NaI, the system exhibited notably different behaviour. Across all the experiments run in this system, the measured voltage difference is higher than the comparable 2 M  $\text{AlCl}_3$  case, and while the reductive current is relatively stable for the 5 M  $\text{AlCl}_3$  with 1 M NaI case, the oxidative current exhibits a stepwise increase in potential as a function of time and current passed. The first, larger step ( $\sim 15$ – $18$  min) and the smaller second step ( $\sim 18$ – $20$  min) are likely the oxidation of partially reduced complexes deposited on the Ni foil electrode. The higher voltage ( $\sim 1.3$  V) step at 20 minutes is seen at by  $0.2$  and  $0.5$  mA  $\text{cm}^{-2}$  current densities and is believed to be related to iodide oxidation,<sup>24</sup> and is not seen in the 2 M  $\text{AlCl}_3$ , 1 M NaI system where the voltages remained low.

Recognizing the promise of the 2 M  $\text{AlCl}_3$ , 1 M NaI system, preliminary half-cell cycling experiments were conducted to explore the stability of the electrolyte and its efficiency over longer charge–discharge cycling under ambient, non-inert conditions. Fig. 5 is a representative trace of the 2 M  $\text{AlCl}_3$ , 1 M NaI electrolyte that was cycled at  $0.2$  mA  $\text{cm}^{-2}$  for 30 min charge/discharge cycles over 24 hours. The potential cycling behaviour



Fig. 3 EDX spectra of Ni foil showing the compositions of deposits formed during deep charge reductions of each electrolyte.



Fig. 4 Potentiometric plots for reduction (0–15 min) and oxidation (15–30 min) at constant current density ( $0.2$  mA  $\text{cm}^{-2}$ ) corresponding to (A) 2 M  $\text{AlCl}_3$  (with and without 1 M NaI) and (B) 5 M  $\text{AlCl}_3$  (with and without 1 M NaI).



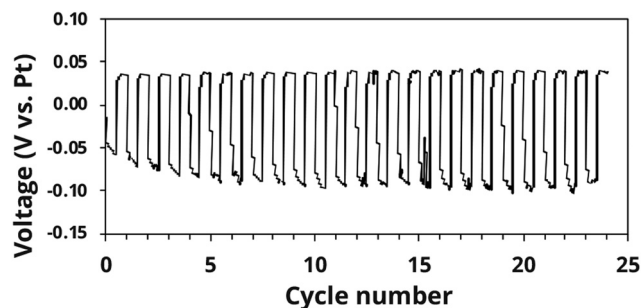


Fig. 5 Electrochemical half-cell cycling profile for 2 M  $\text{AlCl}_3$  with 1 M NaI in EMIM[TFSI] cycled for 30 minutes at  $0.2 \text{ mA cm}^{-2}$ . Working electrode was a 3 mm Ni electrode with separate Pt counter and reference electrodes.

shows promising, relative stable electrochemistry across the 24 cycles. The peak voltage difference in these solutions remains less than 0.15 V for the half-cell. Further cycling and higher depth of discharge experiments will need to be done to determine the maximum performance capacity of this electrolyte. Nevertheless, these preliminary cycling results confirm the relatively low resistance, electrochemically reversible performance of this air-stable aluminium-based electrolyte.

In conclusion an air-stable EMIM[TFSI] IL electrolyte containing  $\text{AlCl}_3$  is described. Notably, air stability is created through the use of a hydrophobic TFSI<sup>-</sup> anion, instead of traditional  $\text{Cl}^-$  anions, but electrochemical activity and reversibility is achieved by preferential substitution of a strongly-binding  $\text{I}^-$  Lewis base instead of bulky TFSI<sup>-</sup> anions in aluminium chloride active material complexes. Introduction of the  $\text{I}^-$  anions leads to the formation of iodide-substituted complexes (e.g.,  $\text{AlCl}_3\text{I}^-$  and  $\text{Al}_2\text{Cl}_6\text{I}^-$ ) which are novel active materials in this hydrophobic IL electrolyte. Importantly, these active materials not only enable reversible, low-overpotential electrochemistry, but they allow electrochemical activity at lower  $\text{AlCl}_3$  concentrations (2 M) than previous recognized (5 M), and these unique species remain soluble during electrochemical reduction. In contrast, TFSI-substituted complexes show little or no electrochemical activity at low  $\text{AlCl}_3$  concentrations and lead to deposition of partially-reduced Al-based complexes at all concentrations. The potential feasibility of the iodide-substituted, air-stable IL electrolyte as a candidate energy storage electrolyte is demonstrated through preliminary half-cell cycling. While further optimization of the system will be required for ultimate utilization, the novelty of this new electrolyte system holds promise for advancing multi-valent aluminium electrochemistry in energy storage.

This material is based on work supported by the U.S. Department of Energy, Office of Electricity (OE), Energy Storage Division. Sandia National Laboratories is a multi-mission laboratory managed and operated by National Technology & Engineering Solutions of Sandia, LLC (NTESS), a wholly owned subsidiary of Honeywell International Inc., for the U. S. Department of Energy's National Nuclear Security Administration (DOE/NNSA) under contract DE-NA0003525. This written work is authored by an employee of NTESS and the employee owns

the right, title and interest in and to the written work and is responsible for its contents. The publisher acknowledges that the U.S. Government retains a non-exclusive, paid-up, irrevocable, world-wide license to publish or reproduce the published form of this written work or allow others to do so, for U.S. Government purposes. Any subjective views or opinions that might be expressed in the written work do not necessarily represent the views of the U. S. Government.

## Data availability

Data collected for this manuscript are managed & maintained by Sandia National Laboratories. The Department of Energy (DOE) will provide public access to results of federally sponsored research in accordance with the DOE Public Access Plan.

## Conflicts of interest

There are no conflicts to declare.

## References

- 1 A. Bakkar and V. Neubert, *Electrochem. Commun.*, 2015, **51**, 113–116.
- 2 Y. Melamed, N. Maity, L. Meshi and N. Eliaz, *Coatings*, 2021, **11**, 1414.
- 3 K. K. Maniam and S. Paul, *Coatings*, 2021, **11**, 80.
- 4 T. Jiang, M. J. Chollier Brym, G. Dubé, A. Lasia and G. M. Brisard, *Surf. Coat. Technol.*, 2006, **201**, 1–9.
- 5 T. Jiang, M. J. Chollier Brym, G. Dubé, A. Lasia and G. M. Brisard, *Surf. Coat. Technol.*, 2006, **201**, 10–18.
- 6 Q. X. Liu, S. Zein El Abedin and F. Endres, *J. Electrochem. Soc.*, 2008, **155**, D357.
- 7 R. Böttcher, S. Mai, A. Ispas and A. Bund, *J. Electrochem. Soc.*, 2020, **167**, 102516.
- 8 M. Shi, J. Jiang and H. Zhao, *Electrochemistry*, 2021, **2**, 185–196.
- 9 J. Robinson and R. A. Osteryoung, *J. Electrochem. Soc.*, 1980, **127**, 122.
- 10 N. Brausch, A. Metlen and P. Wasserscheid, *Chem. Commun.*, 2004, 1552–1553.
- 11 P. Eiden, Q. X. Liu, S. Z. El Abedin, F. Endres and I. Krossing, *Chem. Eur. J.*, 2009, **15**, 3426–3434.
- 12 M. Krebsz, S. Johnston, C. K. Nguyen, Y. Hora, B. Roy, A. N. Simonov and D. R. MacFarlane, *ACS Appl. Mater. Interfaces*, 2022, **14**, 34552–34561.
- 13 T. Liu, Université de Bordeaux, 2014.
- 14 T. Rodopoulos, L. Smith, M. D. Horne and T. Rütger, *Chem. Eur. J.*, 2010, **16**, 3815–3826.
- 15 R. Böttcher, S. Mai, N. Borisenko, A. Ispas, A. Bund and F. Endres, *J. Electrochem. Soc.*, 2023, **170**, 072503.
- 16 Y. C. Lee, J. Kolafa, L. A. Curtiss, M. A. Ratner and D. F. Shriver, *J. Chem. Phys.*, 2001, **114**, 9998–10009.
- 17 A. M. Maraschky, M. L. Meyerson, S. J. Percival, D. R. Lowry, S. Meserole, J. N. Williard, A. S. Peretti, M. Gross, L. J. Small and E. D. Spörke, *J. Phys. Chem. C*, 2023, **127**, 1293–1302.
- 18 R. Y. Lee, S. J. Percival and L. J. Small, *J. Electrochem. Soc.*, 2021, **168**, 126511.
- 19 J. Bouteillon and A. Marguier, *Surf. Technol.*, 1984, **22**, 205–217.
- 20 Y. K. Delimarsky, V. F. Makogon and O. P. Gritsenko, *Ukr. Biokhim. Zh.*, 1980, **46**, 115–118.
- 21 R. L. Falconer, G. S. Nichol, I. V. Smolyar, S. L. Cockcroft and M. J. Cowley, *Angew. Chem., Int. Ed.*, 2021, **60**, 2047–2052.
- 22 M. Mocker, C. Robl and H. Schnöckel, *Angew. Chem., Int. Ed. Engl.*, 1994, **33**, 1754–1755.
- 23 M. Mocker, C. Robl and H. Schnöckel, *Angew. Chem., Int. Ed. Engl.*, 1994, **33**, 862–863.
- 24 K. Tanemoto, G. Mamantov, R. Marassi and G. M. Begun, *J. Inorg. Nucl. Chem.*, 1981, **43**, 1779–1785.

